Tracing Ultrafast Separation and Coalescence of Carrier Distributions in Graphene with Time-Resolved Photoemission

ARTICLE *in* JOURNAL OF PHYSICAL CHEMISTRY LETTERS · JANUARY 2012

Impact Factor: 7.46 · DOI: 10.1021/Jz2014067

8 AUTHORS, INCLUDING:

Georgi L. Dakovski
Stanford University
17 PUBLICATIONS **129** CITATIONS
SEE PROFILE

Tomasz Durakiewicz
National Science Foundation
222 PUBLICATIONS **1,695** CITATIONS
SEE PROFILE

Jian-Xin Zhu
Los Alamos National Laboratory
346 PUBLICATIONS **3,860** CITATIONS
SEE PROFILE

A. D. Mohite
Los Alamos National Laboratory
80 PUBLICATIONS **814** CITATIONS
SEE PROFILE

THE JOURNAL OF PHYSICAL CHEMISTRY Letters

Letter

pubs.acs.org/JPCL

Tracing Ultrafast Separation and Coalescence of Carrier Distributions in Graphene with Time-Resolved Photoemission

Steve Gilbertson,*[,†] Georgi L. Dakovski,[†] Tomasz Durakiewicz,[‡] Jian-Xin Zhu,[§] Keshav M. Dani,[†,⊥] Aditya D. Mohite,[∥] Andrew Dattelbaum,[†] and George Rodriguez[†]

[†]Center for Integrated Nanotechnologies and [‡]Condensed Matter and Magnet Science, Materials Physics and Applications Division, [§]Physics of Condensed Matter and Complex Systems, Theoretical Division, and [∥]Physical Chemistry and Applied Spectroscopy, Chemistry Division, Los Alamos National Laboratory, Los Alamos, New Mexico, United States

Supporting Information

ABSTRACT: Graphene, a recently discovered two-dimensional form of carbon, is a strong candidate for many future electronic devices. There is, however, still much debate over how the electronic properties of graphene behave on ultrashort time scales. Here by employing the technique of time-resolved photoemission, we obtain the evolving quantum distributions of the electrons and holes: on an ultrashort 500 fs time scale, the electron and hole populations can be described by two separate Fermi−Dirac distributions, whereas on longer time scales the populations coalesce to form a single Fermi−Dirac distribution at an elevated temperature. These studies represent the first direct measure of carrier distribution dynamics in monolayer graphene after ultrafast photoexcitation.

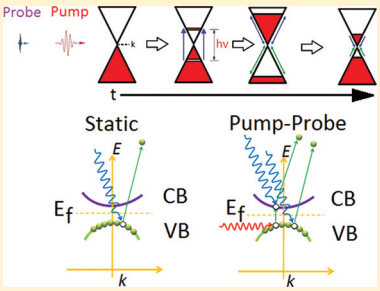

SECTION: Electron Transport, Optical and Electronic Devices, Hard Matter

Since its first experimental demonstration,[1] graphene has quickly become a hot research topic because of its unusual electronic properties and potential in electronic devices.[2−4] The properties of graphene have also led to interesting physical processes like the anomalous quantum Hall effect and Berry phase.[2,5] These unusual properties have attracted significant attention, and much work has already been conducted looking at the static band structure of graphene.[6,7] A question of central importance in time-resolved studies of optoelectronics, particularly high-speed applications, is how the photoexcited carriers behave on ultrashort time scales. Even though more recent time-resolved studies have provided a wealth of information,[8−10] fundamental questions concerning the quantum descriptions of the transient electron−hole plasma remain. More precisely, two alternative views of the dynamical relaxation are possible. For the first possibility, a very rapid thermalization dominated at earliest times (<100 fs) by Coulomb and LO phonon scattering[11] leaves the system of carriers at an elevated temperature, the resultant quasi-equilibrium transient state being described by a Fermi−Dirac distribution given by $F_D = [1 + \exp(\varepsilon - \mu)/kT]^{-1}$ with unaltered chemical potential, μ, but at raised temperature, T. In the above equation, k is Boltzman's constant and ε represents the energy of the electron or hole. We will refer to this system as the T* model. A second possibility is that the resultant quasi-Fermi distributions form transient populations mimicked by two separate Fermi−Dirac distributions with distinctly different chemical potentials and temperatures for the electrons and holes, respectively. We will call this system the μ* model. On one hand, the μ* description of the photoexcited electrons and holes allows for phenomena such as terahertz lasing or using graphene as a saturable absorber in tunable lasers.[12,13] On the other hand, the observation of phenomena such as ultrafast photoluminescence and studies of carrier multiplication in graphene[10,13] imply fundamentally different quantum descriptions of the photoexcited electron-hole plasma, more in line with the T* model. These differences have important implications for using graphene in other applications such as nanoelectronics[14] and sensing[15] and are a consequence of the valence and conduction bands in graphene forming Dirac cones.[16,17]

Ultrafast optical spectroscopy has recently become an important technique for probing electron and phonon dynamics directly in the time domain.[8−10] In both models, the difference between the Fermi−Dirac distribution, ΔF_D, between the pumped and unpumped cases shows qualitative differences in the distributions. (See the Supporting Information.) The parameters used to describe the two different pictures are time-dependent, and their clear determination is crucial for applications. Conductivity, for example, is a strong function of the chemical potential which is quite different between the two models. Additionally, results that imply separate nonzero chemical potentials for the electrons and holes have been previously seen in graphite.[18] Here we improve upon the previous results by using an alternate method to the less direct reflectivity measurements and limited optical pulse energy provided in those experiments to measure carrier dynamics in graphene. The resolution of this problem is

Received: October 20, 2011
Accepted: December 5, 2011

   dx.doi.org/10.1021/jz2014067 | J. Phys. Chem. Lett. 2012, 3, 64−68

difficult to obtain in all-optical experiments where the transient electronic behavior is inferred from changes in the dielectric response function, sensitive to the combined electron−hole response. Nonetheless, the pioneering work concerning carrier dynamics via reflectivity measurements[18] as well as time-resolved photoemission[19] in graphite has set the framework for a more detailed study in graphene. By probing a broad range of low and high energy states with a direct energy spectrum measurement in a single setup, the time-evolution of the electrons and holes can be determined.

We directly measured the energy of the electrons and holes by employing the technique of time-resolved photoemission spectroscopy (PES). Probing the transient distribution of electronic states with high-energy photons allows for distinct monitoring of the electron and hole populations in a true single-particle manner. Here we photoexcited single-layer graphene deposited on a SiO_2 substrate with optical pulses at 1.55 eV and directly probed the electronic states with 30 eV extreme ultraviolet (XUV) photons to photoemit electrons (Supporting Information), obtaining two significant features. First, an energy redistribution of both electrons and holes appears immediately as the pump and probe pulses overlap in time, far exceeding the range implied by the pump photon energy and therefore providing direct evidence of early time redistribution of nonequilibrated carriers via scattering processes on the time scale of the excitation pulse. After this thermalization period, the distribution is quasi-equilibrated, and cannot be explained by the T* model, but agrees very well with the μ* model. Second, qualitatively the μ* picture persists for a few hundred femtoseconds, after which the relaxed electron−hole distributions coalesce into a form that can be more adequately described by the T* model. Such a crossover is possible in graphene due to the specific band structure allowing for extremely rapid carrier thermalization via Coulomb electron−electron and electron−phonon scattering resulting in electron and hole distributions spread over a large energy range. In comparison, such behavior has not been observed in typical metallic zero-gap materials.[20,21] A thorough theoretical description of a physical mechanism for the crossover in graphene is beyond the scope of this work although the complexity of many-body interactions in graphene is currently the focus of ongoing research[22] and may shed more light on this problem in the future. We also repeated the experiment by photoexciting graphene with 3.1 eV pulses and obtained qualitatively the same result.

Our graphene samples were grown on copper through the CVD technique (Supporting Information) and subsequently transferred onto a SiO_2 substrate. SiO_2 was chosen as the substrate to minimize substrate interactions as much as possible due to the large SiO_2 bandgap.[23] Thus created samples were slightly p-doped, but any effects from this were minor compared with the photon energy of the optical pump. This p-doping resulted in a shift of the Fermi energy of ∼200 meV above the Dirac point. Figure 1 shows static photoemission spectra for the substrate with a single graphene layer (black line) and without the graphene (red line). The inset of Figure 1 shows graphene mounted on the SiO_2 substrate after it has been pumped with 1.55 eV photons. The blue line shows the intensity at a negative delay of −500 fs, whereas the green line shows the result at time zero. Also shown is the substrate alone for comparison. Clearly the substrate signal is several orders of magnitude lower than the case of optically pumped graphene included on the substrate. Previous work has also demonstrated

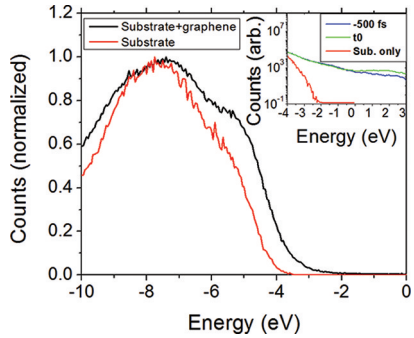

Figure 1. Plots of the static photoemission spectra for graphene on the SiO_2 substrate (black line) and the substrate alone (red line). Zero energy represents the Fermi level. The inset shows the photoemission spectra for a delay of −500 fs (blue line) and at time zero (green line). The spectra are plotted on a Log plot to accentuate differences in the signal near the Fermi edge. Also shown in the inset is the spectrum of the substrate-only (red line) for comparison.

only negligible effects of the substrate on the graphene layer for several different substrates.[24] To ensure that small changes in the charge density due to the optical pump do not induce additional time-dependent doping of the sample, we also pumped the substrate alone, but it exhibited negligible promotion of electrons into the bandgap. Additionally the multidomain nature of the graphene sample meant only photoelectron detection in angle-integrated mode (non-k resolved) was possible.

To reduce thermal effects in the experiment, we cooled the graphene samples to 12 K with a closed-cycle He refrigerator. The near-infrared (1.55 eV) pump pulses used were kept at an absorbed fluence of 0.36 J/m^2.[25] We chose this value as a compromise between a confidently measurable signal and minimal spectral change induced by multiphoton photoemission originating from the intense pump beam. We also repeated the experiment by photoexciting graphene with 3.1 eV ultraviolet pulses of 0.72 J/m^2 absorbed fluence, which ensured a similar number of photons as compared with the 1.55 eV pump. In both cases, the pump beam was stepped in 20 fs delay increments with respect to the probe beam. This was significantly smaller than the dynamics we observed. The recorded PES intensity can be parametrized as the product of a single-particle spectral function, $A(\varepsilon,k)$, a transition matrix-element and the Fermi−Dirac distribution.[26,27] In the limit of angle-integrated detection assuming a constant and momentum-independent matrix element and within the rigid-band approximation, the detected signal is thus proportional to the density of states, $g(\varepsilon)$, (well-known to be a linear function in the vicinity of the Dirac point) and the Fermi−Dirac function, F_D, with the dynamic behavior of photoexcited electrons and holes entirely mimicked by a modified temperature, chemical potential, or both. It should be stated that assuming a constant matrix element is valid only if the carrier distribution is isotropic. During the first few tens of femtoseconds after optically exciting graphene, equilibration of the carriers results in an anisotropic distribution. A more detailed description of the carrier distributions during this initial period is a subject of theoretical work.[28−32] This approach has been successful in explaining transient electronic structure both in simple metals and in more complex materials.[33−35]

In Figure 2, we plot the difference in Fermi−Dirac distributions of the pumped and unpumped case, ΔF_D, of the

dx.doi.org/10.1021/jz2014067 | J. Phys. Chem. Lett. 2012, 3, 64−68

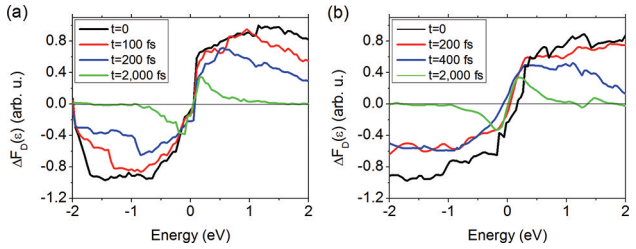

Figure 2. Experimental ΔF_D at different delays for (a) 1.55 and (b) 3.1 eV pump photon energy. The data shown are the difference of the experimentally obtained pumped spectrum (T > 12 K) and the unpumped spectrum (T = 12 K) divided by the linear density of states function. Near t = 0, the shape mimics the μ^* case, whereas at later time delays the behavior more closely resembles the T* case. The transition between the μ^* and T* case does not occur at a well-defined delay, so for clarity a delay of 2 ps is chosen to demonstrate the T* behavior.

photoelectron spectra recorded at increasing temporal delays between the pump and probe pulses for (a) 1.55 and (b) 3.1 eV pump energies. In all cases, a spectrum at large negative delay was subtracted as the low temperature case, and the resultant spectrum was divided by a fixed linear function simulating the density of states of graphene, $g(\varepsilon)$. Values of $g(\varepsilon)$ near zero energy were omitted to avoid discontinuities. This changed the results shown in Figure 2 in a minimal way because we are mainly concerned with the data >200 meV away from zero. The different traces in Figure 2 therefore represent the time evolutions of the excess electron and hole probability distributions following photoexcitation. Qualitatively, we observe that within the limits of our time resolution (20 fs) both distributions extend well beyond the 0.78 eV (1.55 eV) value expected from the pump photon energy of 1.55 eV (3.1 eV). On this extremely short time scale, the Coulomb electron−electron interaction is the dominant candidate responsible for this initial intraband energy redistribution[29,30] with contributions from electron−phonon interactions.[9] This is in contrast with similar studies on metallic systems where the unique band structure of graphene plays a crucial role.[20] Previous work has predicted electron−electron scattering times on the order of 10 fs for electron densities of ∼10^{12} cm^{-2};[19] however, the time scale would be even shorter due to the larger electron density of 10^{14} cm^{-2} present in our experiments due to our high fluence. As a result of reduced scattering due to a small phase-space in the vicinity of the Dirac point, the longest lived quasiparticle states are found within the linear density of states. This behavior, coupled to the extremely high mobility, leads to transient electron and hole populations almost instantaneously occupying an unusually large portion in energy-momentum space. Turning to a more quantitative analysis of the excess carrier distributions, we begin by noting that an attempt to fit the experimental data in the first 500 fs to the T* model leads to an obvious qualitative discrepancy with the obtained results. On the contrary, within the μ^* model, the excess carriers' chemical potentials and temperatures can be directly calculated from the photoexcited electron and hole densities (assumed equal to the density of absorbed photons), and are seen to match the results at zero delay remarkably well. This implies that the strong electron−electron and electron−phonon interactions guarantee an efficient thermalization of the excess populations and the approach of assigning Fermi−Dirac distribution(s) after the initial thermalization process (50−100 fs) is therefore a valid one. However, the theoretical determination of the four parameters μ_e, μ_h, T_e, and T_h in the μ^* model at later delay times can be obtained only if the excess carriers and heat time-evolution ($T_e(t)$ and $T_h(t)$) are known, which is a task beyond the scope of this work. Rather, by fitting the data at increasing delay times to the μ^* model, we extract the temporal behavior (Figure 3) of the four parameters. (For

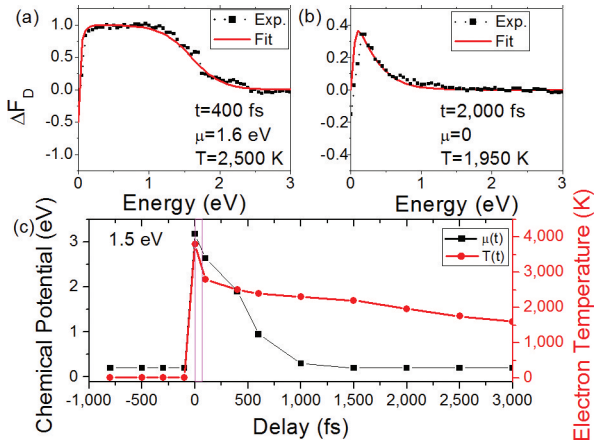

Figure 3. Fitting of the experimental data (black squares) with ΔF_D (red line) for a 1.5 eV pump pulse at delays of (a) t = 400 fs and (b) t = 2000 fs. Only the electrons are fitted because the data do not have perfect symmetry between the electrons and holes because of p-doping of the sample. For delays closer to time zero (see panel a), the fitting cannot be accomplished without the inclusion of a nonzero chemical potential. At later delays (b), the chemical potential can be zero and still achieve fitting. The values of T (red circles) and μ (black squares) for several delay values are plotted in panel c. The shape of $T(t)$ is similar to results of the two-temperature model, whereas $\mu(t)$ could not be measured in previous experiments.[7] Also shown is the region of delay where equilibration occurs, and hence the values of T and μ are invalid. This is shown as a vertical red rectangle near delay zero.

simplicity, we assume $\mu_e = \mu_h$ and $T_e = T_h$, although in reality there is an asymmetry between the electrons and holes that we attribute to p-doping of the sample).

In fact, the temperature variation is seen to follow a trend in agreement with previous experiments, namely, a very rapid decrease in the first 100 fs, attributed to strong electron−electron and electron−phonon coupling, followed by a bottleneck effect leading to relaxation on a much longer picosecond scale principally determined by carrier-phonon scattering during electron−hole recombination.[10] It should be noted, however, that intraband scattering requires a few tens of femtoseconds to thermalize the system, and as such the Fermi function during this time is not valid. This time scale where the dynamics are unknown is shown as a vertical red rectangle in Figure 3c. The chemical potentials assigned to the excess carrier distributions have values significantly different from zero and are seen to rapidly decrease (in magnitude). After ∼1 ps they are equal to zero, indicating the complete crossover to a state described by the T* model with electron and hole distributions in chemical and elevated temperature equilibrium. Previous work has shown that the electron−hole densities play a major role in the recombination rates and hence the measured lifetimes of the electron−hole pairs.[28−32] Auger recombination and impact ionization both contribute to the generation and eventual recombination rate of the electron−hole pairs, and it is expected that increasing the number of carriers present can reduce the lifetime.[28] The results for the 3.1 eV pump pulse

dx.doi.org/10.1021/jz2014067 | J. Phys. Chem. Lett. 2012, 3, 64−68

qualitatively agree with the 1.55 eV results, as indicated by the previously observed behavior in Figure 2. For the 3.1 eV pump case, as seen in Figure 2b, the electron and hole chemical potentials are seen to extend to even larger (in absolute value) energies, while relaxing together with the temperature on similar time scales. We wish to emphasize that the goal of this study was to track qualitatively the transient behavior of photoexcited graphene mounted on SiO_2. In particular, we expect that relaxation times would be different depending on sample preparation, excitation fluence, and other experimental conditions.

Another way of analyzing the data is to look at the temporal, rather than spectral, domain and take advantage of the ultrashort time resolution offered by time-resolved PES. In Figure 4a, we show the time evolution of the excess electrons

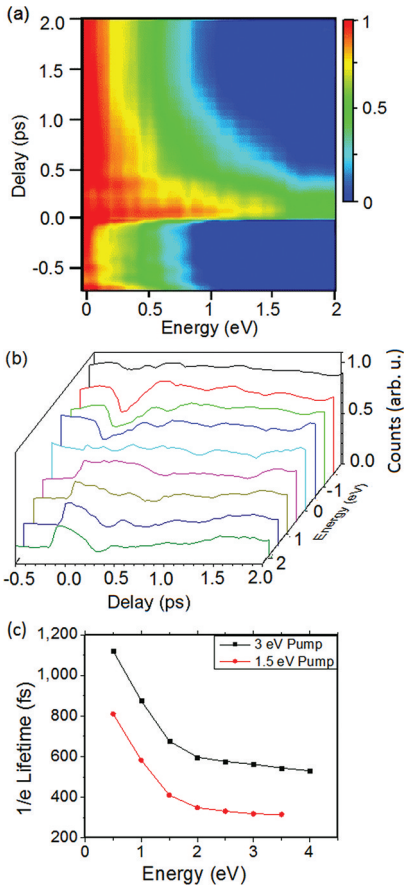

Figure 4. (a) Surface plot of the energy spectra of the electrons as a function of delay for graphene pumped with 1.55 eV photons. (b) Lineout plots across the delay axis of (a) for various energies. (c) Measured 1/e decay times of the electrons are shown for 1.55 eV (red circles) and 3 eV (black squares) pump photon energy.

photoexcited with a 1.55 eV pump beam and residing at different electronic states. Figure 4b shows lineout plots at various energies both above and below zero energy. A peak is present at values above zero, representing promoted carriers above the Fermi edge, whereas a dip in the population from hole generation is seen for values below zero. By fitting these dynamical processes with an exponential function, we extract the lifetime of optically excited quasiparticles as a function of their energy, as shown in Figure 4c. The general trend of the decreasing scattering rate as one approaches the Dirac point can be understood in terms of a reducing phase space volume, resulting in longer-lived low-energy excitations. This trend has already been observed implicitly in two-pulse photoluminescence measurements, in agreement with our results.[10] Again, by using a 3.1 eV pump beam, we observed qualitatively similar behavior with slightly increased lifetimes (Figure 4b) reflecting the larger spread of excess carrier distributions and correspondingly longer times necessary to relax to the ground state. Previous work has already measured the quasiparticle lifetimes in graphite, although the results probed levels only 0.15 eV above the work function of the sample,[19] limiting the emitted photoelectron energy spectrum to <1 eV. By using XUV photons, the full energy spectrum of excited carriers and the corresponding holes in graphene can be probed directly and in a time-resolved manner. In our experiments, we have been able to measure the lifetimes at a very high- and low-energy region simultaneously, in contrast with previous experiments.[18] The low-energy results can be fit nicely with a Dirac fermion model with a linear energy dispersion (see the Supporting Information for details), suggesting that our experiments are revealing the uniqueness of graphene. The measured lifetimes near the Fermi edge in graphite were measured to be ~250 fs,[19] which is significantly shorter, although on the same order of magnitude, as the lifetime of ~800 fs (for 1.55 eV case) measured in the same energy range in graphene, as seen in Figure 4b. The difference between the two cases could be due possibly to decreased lattice interactions in graphene as compared with graphite.

The observation of this nontrivial behavior of optically excited graphene is of primary importance for numerous proposed applications of this material. Changes from the μ^* to the T* model after an ultrafast time scale have broad implications in a number of phenomena,[7−10] and because a crossover is directly observed, time-dependent properties of graphene must be considered in applications.[12−15] These results do not significantly contradict previous reflectivity and transmissivity studies in graphite,[18] even with the more direct measurement of the electron and hole distributions in time-resolved PES and with the higher energy states probed with our method. The band structure of graphene, ultimately responsible for this unique rearrangement of the electron−hole plasma, indicates that materials with similar Dirac structure of linear dispersion and zero-gap, such as topological insulators, may behave in a similar manner upon photoexcitation. In addition, adding the spin degree of freedom in the excitation process may lead to even more technological applications. The technique of time-resolved photoemission seems to be an ideal candidate to track the electronic states simultaneously in the energy, momentum, and time domains.

■ ASSOCIATED CONTENT

Supporting Information

Detailed information concerning experimental procedures, data analysis techniques, examples of raw data, and theoretical calculations. This material is available free of charge via the Internet at http://pubs.acs.org.

■ AUTHOR INFORMATION

Corresponding Author

*E-mail: steveg@lanl.gov.

dx.doi.org/10.1021/jz2014067 | J. Phys. Chem. Lett. 2012, 3, 64−68

Present Address

[⊥]Femtosecond Spectroscopy Unit, Okinawa Institute of Science and Technology, Okinawa, Japan.

■ ACKNOWLEDGMENTS

Funding for this work was provided by the Laboratory Directed Research and Development program at Los Alamos National Laboratory under the auspices of the Department of Energy for Los Alamos National Security LLC under contract no. DE-AC52-06NA25396. We thank the Center for Integrated Nanotechnologies for providing the graphene samples used in this work.

■ REFERENCES

(1) Novoselov, K. S.; Geim, A. K.; Morozov, S. V.; Jiang, D.; Zhang, Y.; Dubonos, S. V.; Grigorieva, I. V.; Firsov, A. A. Electric Field Effect in Atomically Thin Carbon Films. *Science* **2004**, *306*, 666−669.

(2) Zhang, Y.; Tan, Y.; Stormer, H. L.; Kim, P. Experimental Observation of the Quantum Hall Effect and Berry's Phase in Graphene. *Nature* **2005**, *438*, 201−204.

(3) Peres, N. M. R.; Guinea, F.; Castro Neto, A. H. Electronic Properties of Disordered Two-Dimensional Carbon. *Phys. Rev. B* **2006**, *73*, 125411.

(4) Gusynin, V. P.; Sharapov, S. G. Unconventional Integer Quantum Hall Effect in Graphene. *Phys. Rev. Lett.* **2005**, *95*, 146801.

(5) Bolotin, K. I.; Ghahari, F.; Shulman, M. D.; Stormer, H. L.; Kim, P. Observation of the Fractional Quantum Hall Effect in Graphene. *Nature* **2009**, *462*, 196−199.

(6) Ohta, T.; Bostwick, A.; Seyller, T.; Horn, K.; Rotenberg, E. Controlling the Electronic Structure of Bilayer Graphene. *Science* **2006**, *313*, 951−954.

(7) Zhou, S. Y.; Gweon, G. H.; Fedorov, A. V.; First, P. N.; De Heer, W. A.; Lee, D. H.; Guinea, F.; Castro Neto, A. H.; Lanzara, A. Substrate-Induced Bandgap Opening in Epitaxial Graphene. *Nat. Mater.* **2007**, *6*, 770−775.

(8) Sun, D.; Wu, Z.; Divin, C.; Li, X.; Berger, C.; de Heer, W. A.; First, P. N.; Norris, T. B. Ultrafast Relaxation of Excited Dirac Fermions in Epitaxial Graphene Using Optical Differential Transmission Spectroscopy. *Phys. Rev. Lett.* **2008**, *101*, 157402.

(9) Breusing, M.; Kuehn, S.; Winzer, T.; Malic, E.; Milde, F.; Severin, N.; Rabe, J. P.; Ropers, C.; Knorr, A.; Elsaesser, T. Ultrafast Nonequilibrium Carrier Dynamics in a Single Graphene Layer. *Phys. Rev. B* **2011**, *83*, 153410.

(10) Lui, C. H.; Mak, K. F.; Shan, J.; Heinz, T. F. Ultrafast Photoluminescence from Graphene. *Phys. Rev. Lett.* **2010**, *105*, 127404.

(11) Winzer, T.; Knorr, A.; Malic, E. Carrier Multiplication in Graphene. *Nano Lett.* **2010**, *10*, 4839−4843.

(12) Sun, Z.; Popa, D.; Hasan, T.; Torrisi, F.; Wang, F.; Kelleher, E. J. R.; Travers, J. C.; Nicolosi, V.; Ferrari, A. C. A Stable, Wideband Tunable, Near Transform-Limited, Graphene-Mode-Locked, Ultrafast Laser. *Nano Res.* **2010**, *3*, 653−660.

(13) Ryzhii, V.; Ryzhii, M.; Satou, A.; Otsuji, T.; Dubinov, A. A.; Aleshkin, V. Y. Feasability of Terahertz Lasing in Optically Pumped Epitaxial Multiple Graphene Layer Structures. *J. Appl. Phys.* **2009**, *106*, 084507.

(14) Berger, C.; Song, Z.; Li, X.; Wu, X.; Brown, N.; Naud, C.; Mayou, D.; Li, T.; Hass, J.; Marchenov, A.; et al. Electronic Confinement and Coherence in Patterned Epitaxial Graphene. *Science* **2006**, *312*, 1191−1196.

(15) Schedin, F.; Geim, A. K.; Morozov, S. V.; Hill, E. W.; Blake, P.; Katsnelson, M. I.; Novoselov, K. S. Detection of Individual Gas Molecules Adsorbed on Graphene. *Nat. Mater.* **2007**, *6*, 652−655.

(16) Park, C. H.; Giustino, F.; Spataru, C. D.; Cohen, M. L.; Louie, S. G. Angle-Resolved Photoemission Spectra of Graphene from First-Principles Calculations. *Nano Lett.* **2009**, *9*, 4234−4239.

(17) Bostwick, A.; Ohta, T.; Seyller, T.; Horn, K.; Rotenberg, E. Quasiparticle Dynamics in Graphene. *Nat. Phys.* **2007**, *3*, 36−40.

(18) Breusing, M.; Ropers, C.; Elsaesser, T. Ultrafast Carrier Dynamics in Graphite. *Phys. Rev. Lett.* **2009**, *102*, 086809.

(19) Moos, G.; Gahl, C.; Fasel, R.; Wolf, M.; Hertel, T. Anisotropy of Quasiparticle Lifetimes and the Role of Disorder in Graphite from Ultrafast Time-Resolved Photoemission Spectroscopy. *Phys. Rev. Lett.* **2001**, *87*, 267402.

(20) Siffalovic, P.; Drescher, M.; Spieweck, M.; Wiesenthal, T.; Lim, Y. C.; Weidner, R.; Elizarov, A.; Heinzmann, U. Laser-Based Apparatus for Extended Ultraviolet Femtosecond Time-Resolved Photoemission Spectroscopy. *Rev. Sci. Instrum.* **2001**, *72*, 30−35.

(21) Petek, H.; Ogawa, S. Femtosecond Time-Resolved Two-Photon Photoemission Studies of Electron Dynamics in Metals. *Prog. Surf. Sci.* **1997**, *56*, 239−310.

(22) Siegel, D.; Park, C.; Hwang, C.; Deslippe, J.; Fedorov, A. V.; Loie, S. G.; Lanzara, A. Many-Body Interactions in Quasi-Freestanding Graphene. *Proc. Natl. Acad. Sci. U.S.A.* **2011**, *108*, 11365−11369.

(23) Knox, K. R.; Wang, S.; Morgante, A.; Cvetko, D.; Locatelli, A.; Mentes, T. O.; Nino, M. A.; Kim, P.; Osgood, R. M. Jr. Spectromicroscopy of Single and Multilayer Graphene Supported by a Weakly Interacting Substrate. *Phys. Rev. B* **2008**, *78*, 201408(R).

(24) Wang, Y.; Ni, Z.; Yu, T.; Shen, Z. X.; Wang, H.; Wu, Y.; Chen, W.; Wee, A. T. S. Raman Studies of Monolayer Graphene: The Substrate Effect. *J. Phys. Chem. C* **2008**, *112*, 10637−10640.

(25) Falkovsky, L. A.; Pershoguba, S. S. Optical Far-Infrared Properties of a Graphene Monolayer and Multilayer. *Phys. Rev. B* **2007**, *76*, 153410.

(26) Hufner, S. *Photoelectron Spectroscopy*, 2nd ed.; Springer: Berlin, 1996.

(27) Rossnagel, K.; Kipp, L.; Skibowski, M.; Solterbeck, C.; Strasser, T.; Schattke, W.; VoB, D.; Kruger, P.; Mazur, A.; Pollman, J. Three-Dimensional Fermi Surface Determination by Angle-Resolved Photoelectron Spectroscopy. *Phys. Rev. B* **2001**, *63*, 125104.

(28) Rana, F. Electron Hole Generation and Recombination Rates for Coulomb Scattering in Graphene. *Phys. Rev. B.* **2007**, *76*, 155431.

(29) Malic, E.; Winzer, T.; Bobkin, E.; Knorr, A. Microscopic Theory of Absorption and Ultrafast Many-Particle Kinetics in Graphene. *Phys. Rev. B.* **2011**, *84*, 205406.

(30) Winzer, T.; Malic, E. Microscopic Study of the Efficiency of Coulomb and Phonon Induced Relaxation Channels in Graphene. *Phys. Status Solidi B.* **2011**, *248*, 2615−2618.

(31) Kim, R.; Perebeinos, V.; Avouris, P. Relaxation of Optically Excited Carriers in Graphene. *Phys Rev. B.* **2011**, *84*, 075449.

(32) Rana, F.; Strait, J. H.; Wang, H.; Manolatou, C. Ultrafast Carrier Recombination and Generation Rates for Plasmon Emission and Absorption in Graphene. *Phys. Rev. B.* **2011**, *84*, 045437.

(33) Schoenlein, R. W.; Lin, W. Z.; Fujimoto, J. G.; Eesley, G. L. Femtosecond Studies of Nonequilibrium Electronic Processes in Metals. *Phys. Rev. Lett.* **1987**, *58*, 1680.

(34) Perfetti, L.; Loukakos, P. A.; Lisowski, M.; Bovensiepen, U.; Eisaki, H.; Wolf, M. Ultrafast Electron Relaxation in Superconducting $Bi_2Sr_2CaCu_2O_{8+\delta}$ by Time-Resolved Photoelectron Spectroscopy. *Phys. Rev. Lett.* **2007**, *99*, 197001.

(35) Gianetti, C.; Coslovich, G.; Cilento, F.; Ferrini, G.; Eisaki, H.; Kaneko, N.; Greven, M.; Parmigiani, F. Discontinuity of the Ultrafast Electronic Response of Underdoped Superconducting $Bi_2Sr_2CaCu_2O_{8+\delta}$ Strongly Excited by Ultrashort Light Pulses. *Phys. Rev. B* **2009**, *79*, 224502.